

PHYSICAL PROPERTIES OF COMETARY DUST

J.A.M. McDONNELL
Unit for Space Sciences
University of Kent
Canterbury, Kent, U.K.

P.L. LAMY
Laboratoire
d'Astronomie Spatiale
CNRS, Les Trois Lucs
13012 Marseille, France

G.S. PANKIEWICZ
Unit for Space Sciences
University of Kent
Canterbury, Kent, U.K.

ABSTRACT. Prior to the 1986 apparition of comet Halley, all attempts to determine the physical properties of cometary dust were limited to remote observations and the analysis of various particles captured by the Earth's atmosphere. The *in situ* measurements made by the three spacecraft that passed within 10,000 km of the nucleus provided the first opportunity to investigate both the full size-range of particles and the complete process of dust production. Information on composition is derived through mass spectra and the scattering and emission of light from the grains, whilst the dynamics of the dust coma can be modeled from the three separate sets of measurements made over a period of eight days.

1. Properties Deduced From *In Situ* Impact Detectors

1.1. INTRODUCTION

Although remote measurements traditionally form the basis for cometary observations, the data so gathered concerning the local distribution of dust within the inner coma are necessarily smeared by the line-of-sight integration of any feature and degraded by the limiting resolution of the instrument.

This introduces spatial confusion in the three axes, which is amplified when the *interpretation* of the observed parameters is attempted. Deconvolution of, for example, the observed brightness into the local particulate number density involves knowledge of the size distribution, which is changing perhaps both spatially and temporally, and also of the albedo. The first part of this review summarizes aspects of the direct observation of instrument impact rates, together with their amplitude and time distributions, in order to define the local concentration of dust grains. Such number densities may then be used directly to infer (under assumed or known properties of the dynamics of the dust) nucleus emission characteristics (Section 1.7) and to resolve ambiguities with remote data (Section 2). A full understanding requires, as we shall see, compatibility with the complete suite of instruments on the three spacecraft (Giotto, VEGA 1 and VEGA 2) and Earth-based data. Such understanding is yet far from complete!

1.2. FLUX RATES FROM *IN SITU* MEASUREMENTS

In the first encounter with a comet by the serendipitous exploitation of the International Sun Earth Explorer (ISEE) 2 spacecraft, no dust detectors were available, and hence only upper limits of the dust density were deduced. These upper limits were not out of line with modelling then current (von Roseninge *et al.*, 1986, summarizes the mission).

VEGA 1's three primary impact detectors thus provided first proof of the unique effectiveness of *in situ* detection, commencing from a cometocentric distance of 320,000 km. Representative data from the first published results are shown for the VEGA SP-1 detector in Figure 1 (Vaisberg *et al.*, 1987), for the SP-2 detector, shown here for VEGA 2, in Figure 2 (Mazets *et al.*, 1987) and for the Dust Counter and Mass Analyser (DUCMA) detector on VEGA 1 and 2 in Figure 3 (Simpson *et al.*, 1986).

Flux data obtained from the Particulate Impact Analyser (PIA) (Kissel, 1986), flown as PUMA on VEGA 1 and 2 and PIA on Giotto, are incorporated in the joint presen-

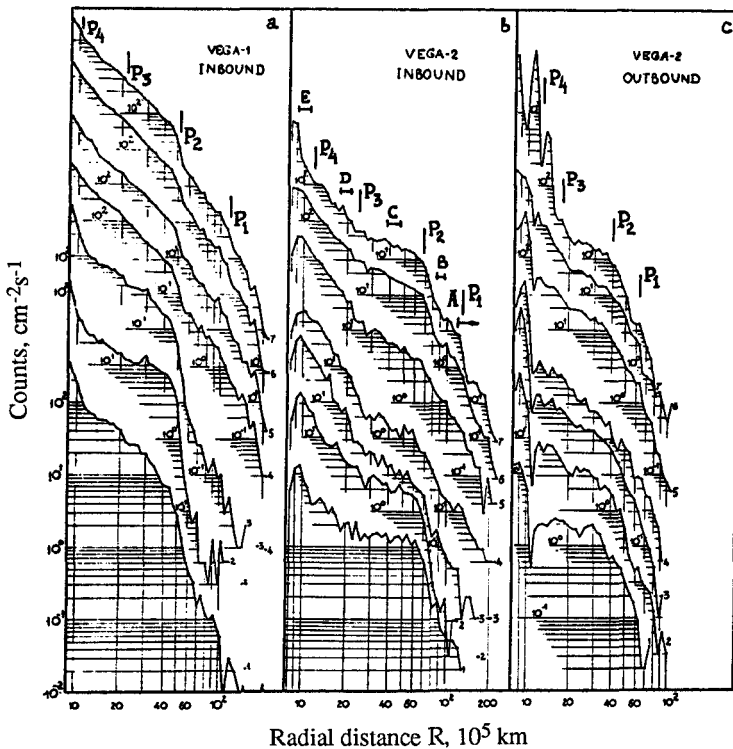


Figure 1. Counts of dust impacts are shown as a function of cometocentric distance measured during the first encounters with comet Halley by VEGA 1 and VEGA 2 on March 6 and 9, 1986. The counts were recorded on the plasma-sensing instrument SP-1 (Vaisberg *et al.*, 1987).

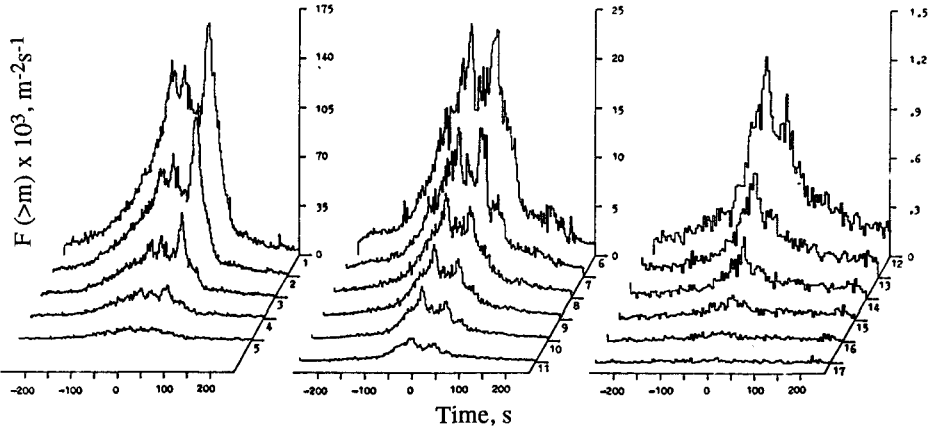


Figure 2. Flux-time profiles measured by the SP-2 instrument on VEGA 2 (Mazets *et al.*, 1987) are shown as a function of time from closest approach (in seconds), which was 8,030 km, comparable with the 8,890 km for VEGA 1 (Sagdeev *et al.*, 1986). The SP-2 detector incorporated a plasma sensor (channels 1 to 5) and acoustic (6 to 17) sensors.

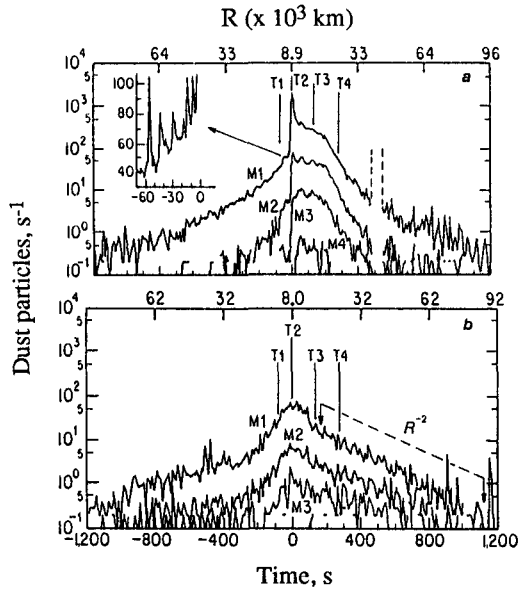


Figure 3. The DUCMA experiment flow on the VEGA spacecraft used a new depolarization detector for dust impacts, and results are given here for both flybys (Simpson *et al.*, 1986). The large surge just before closest approach on VEGA 1 (top) is particularly striking, especially as neither SP-1 nor SP-2 recorded a similar phenomenon.

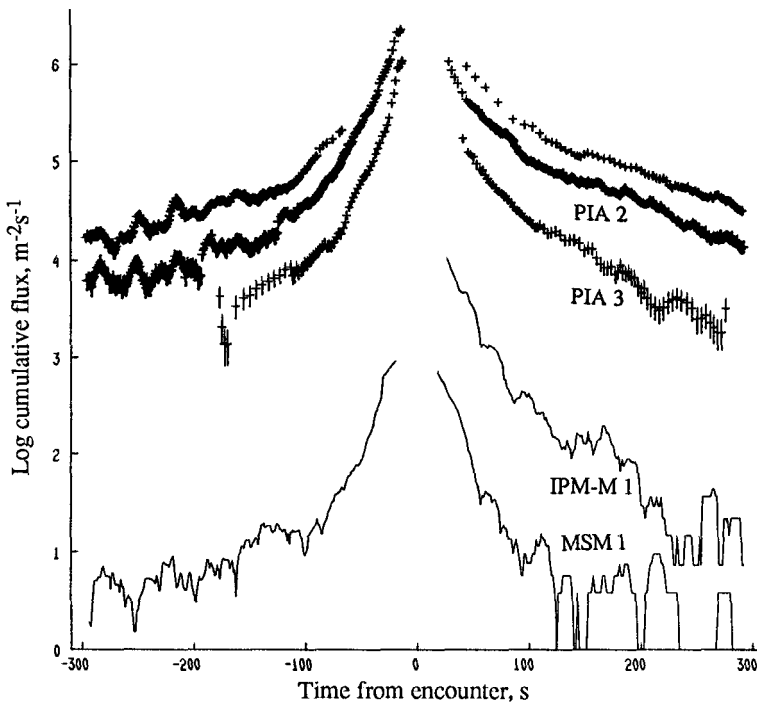


Figure 4. Giotto PIA and DIDSY flux rates are given for masses ranging from 10^{-19} to $\sim 10^{-11}$ kg. Asymmetry in small particle fluxes pre- and post-encounter is clear, as are significant jet features in higher mass channels (McDonnell *et al.*, 1989a).

tation with Dust Impact Detection System (DIDSY) flux rates in Figure 4. Implications of the mass spectra have been discussed more recently in publications by Jessberger *et al.* (1988). The elemental analysis of microparticles on the three spectrometers has provided rich data, and, in fact, new dimensions of research on the cosmogenic scenario for the understanding of the early Solar System; the 'missing carbon' discovered within the CHON particles at last answers the question raised by Delsemme (1977) and a number of workers at earlier times. Previous to the close encounters, it was not known that such carbon could be locked up in the grains—our nearest entities available for terrestrial analysis had been the stratospherically collected Brownlee particles. Even the chondritic porous grains, though, have by this time lost the rich but yet undefined ingredient giving the CHON signatures close to the comet (Brownlee, 1988).

Flux data, leading on the spacecraft to an amplitude distribution over any particular period, have been reduced to an equivalent *mass* distribution using calibrations made available from electrostatic hypervelocity accelerator facilities (McDonnell, 1987) and plasma drag accelerators (Igenbergs and Kuczera, 1979). Such calibrations are, we must admit, not likely to be realistic of the impact of (especially) the porous agglomerates impacting at

68 to 79 km·s⁻¹ for the three spacecraft encounters. However, at such high velocities, the principle of late stage equivalence in cratering theory (Whipple 1958) does substantially reduce the dependence of target response to uncertainties of both projectile density and profile. There were a variety of techniques used in the three missions, namely:

- (i) Impact plasma ionization—PUMA, PIA, SP-1, SP-2, DIDSY (IPM-P).
- (ii) Piezoelectric momentum sensing—DIDSY, SP-1, SP-2.
- (iii) Penetration sensing—DIDSY (RSM).
- (iv) Capacitor discharge sensing—DIDSY (CIS).
- (v) Dielectric film depolarization—DUCMA (PVDF).

Deployment of combinations of these various techniques on the three spacecraft (some making simultaneous detection of the same particles), and subsequent harmonization of remaining calibration uncertainties have probably led to a mass calibration more effective than many other uncertainties or measurements.

The detection techniques used generally rely on threshold sensing to determine the cumulative number of impacts above the given mass; a slightly higher mass threshold, perhaps obtained from the impact amplitude, may provide differential count rate information. An exception to the rule included the large-area acoustic sensors of DIDSY, for which the response falls off as a function of impact-sensor distance, and for which an effective area and corresponding most probable mass must be determined. The VEGA SP-2 detectors, making use of plasma and acoustic sensors with overlapping thresholds, effectively calibrated the charge-to-mass ratio and momentum enhancement, with values of 10⁶ C kg⁻¹ and 10, respectively. For information on the particle density, we refer to Section 1.3 and to Section 2.

The resultant flux-mass distributions observed at Halley were certainly not static in their form; Figure 5 shows five distributions ranging from 8,900 km to the integrated region around 130,000 km after closest approach for VEGA 1's flyby (Mazets *et al.*, 1987). The use of both plasma and acoustic sensing to increase the mass range shows significant fluctuations over the largest and smallest mass regimes. DIDSY data from 'binned' and discrete counts (from which individual particle masses up to ~ 10⁻⁵ kg were recorded), combined with PIA rates, where masses may be as small as 10⁻¹⁹ kg, are shown in Figure 6 over two periods pre- and post-encounter during the Giotto encounter. The relatively large number of large grains pre-encounter is clear, balanced by a converse trend for the smallest particles.

1.3. THE NATURE OF THE IMPACTING DUST

Prior to *in situ* encounters with comet Halley, the most significant comet particulate related compositional information was derived in a second-hand way through laboratory studies of particles collected in the Earth's stratosphere. As pointed out in Section 1.2, the CHON particles, discovered by time-of-flight mass spectrometry on the three flybys, indicate this to be the missing component from the fluffy chondrites.

Ions resulting from the high-velocity impacts at 79 km·s⁻¹ and their energy distribution showed that most dust particles recorded by PUMA-1 (on VEGA 1), flying through the dustiest coma environment, consist of a fluffy silicate core, covered by refractory, icy organics, which, in turn, are also fluffy (Kissel and Krueger, 1987). Spectra from the PIA instrument also provide typical examples of this bimodal dust population. Figure 7 shows a silicate-rich spectrum of a classical rock-forming grain, containing large abundances of C,

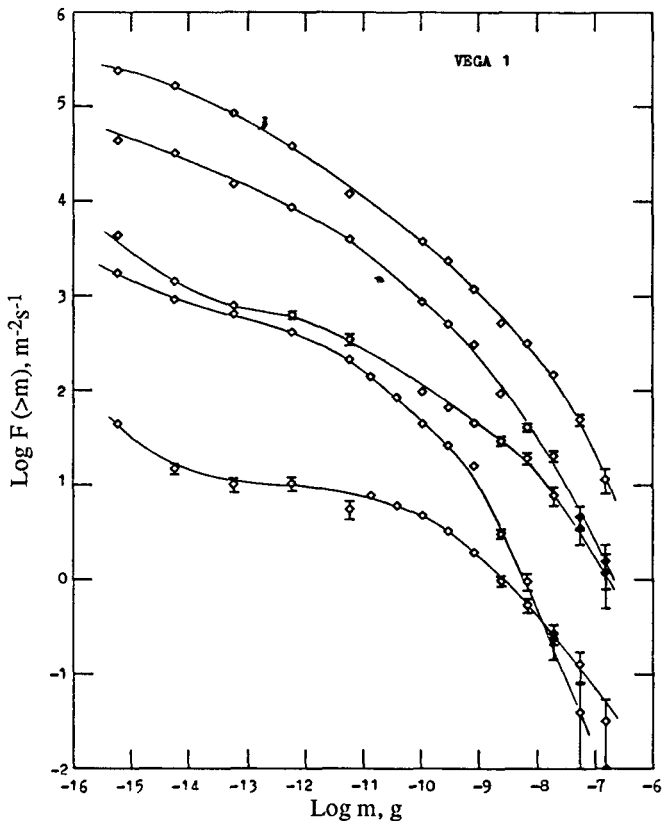


Figure 5. The cumulative flux distributions measured by the SP-2 experiment on VEGA 1 post-encounter show their changing nature (Mazets *et al.*, 1987). Distributions were taken at 8,900 km (top), 12,000 km, 37,000 km, 40,000 to 80,000 km and 80,000 to 180,000 km.

Mg, S, Ca and Fe. Also shown is a spectrum from a CHON particle: a sample of Halley's organic refractory component before processing in the outer coma or in interplanetary space.

Comparisons of impacting Halley dust have been made to carbonaceous CI type chondrites (the most unaltered early Solar System material available for laboratory analysis), with average compositions agreeing to within a factor of two, but with exceptions for the very light and volatile elements, which have lower abundances in the chondrites (Jessberger *et al.*, 1988). The enrichment of CHON-type grains observed in Halley's dust therefore identifies it as the most primitive material yet analyzed *in situ*.

There may therefore be a strong possibility that comets do contain pre-solar interstellar grains. The Greenberg model (1982) of elongated core-mantle interstellar grains as resembling cometary grains certainly predicts the high carbon content and organic mantling.

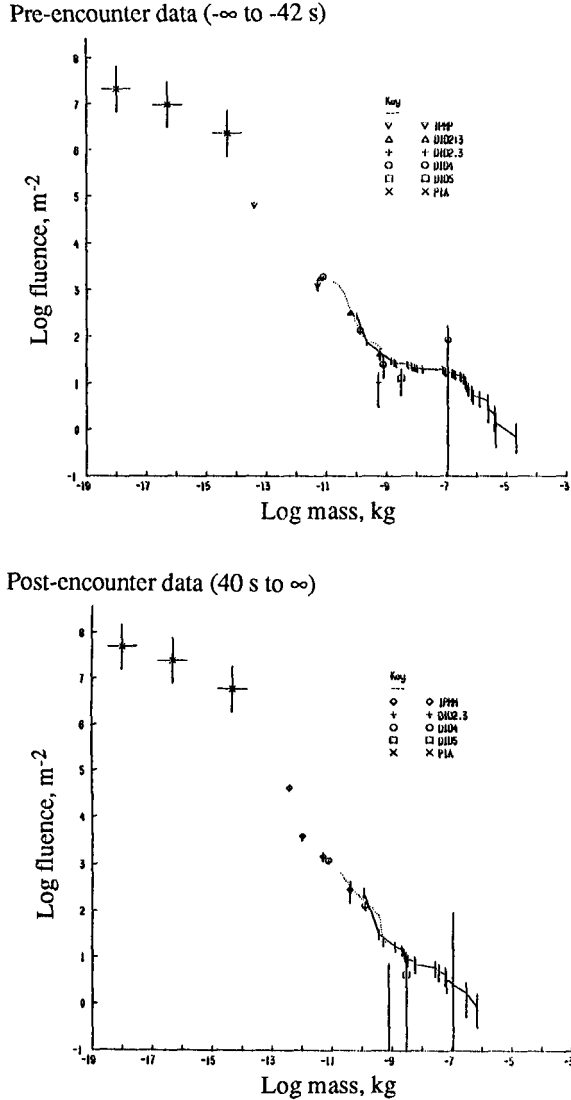


Figure 6. Two cumulative flux distributions from Giotto are integrated out from 2,900 km pre- and post-encounter for PIA, DIDSY binned and DIDSY discrete data (McDonnell *et al.*, 1989b).

However, carbon richness is common to all models for interstellar matter, and a third of Halley particles are composed almost entirely of silicate materials with no organic mantle. Processing during or after the formation of Halley might be required, but Brownlee (1988) has pointed out that “to state that Halley is actually composed of interstellar grains all hav-

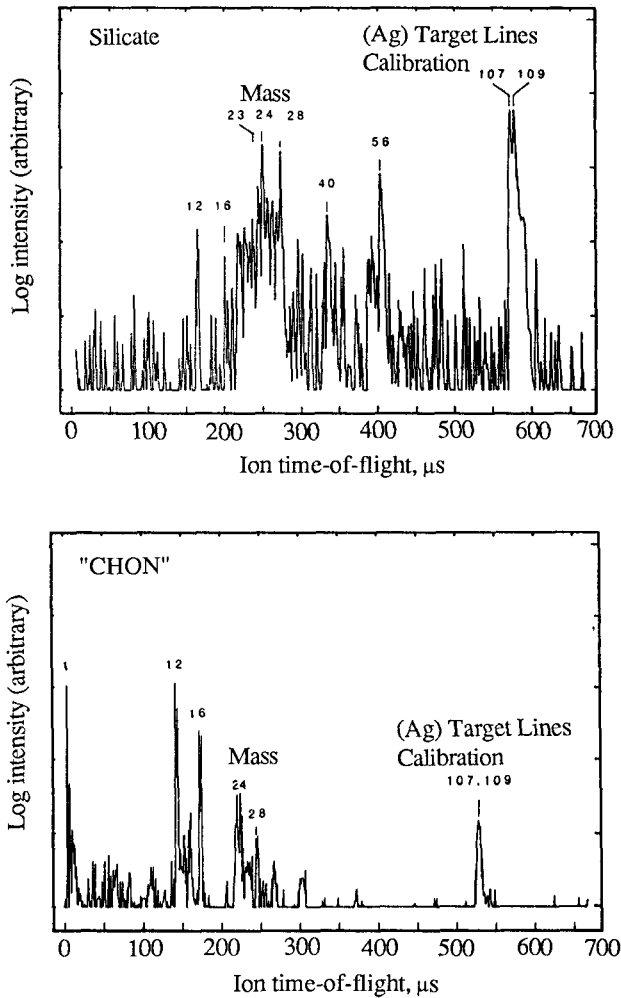


Figure 7. Impact spectra from the Giotto PIA instrument are shown. Two particle types are illustrated (J. Kissel, MPI-H), namely the silicate and carbonaceous CHON classes.

ing core-mantle structure would be a gross overinterpretation." Investigations of the 3.4- μm and 9.7- μm thermal emission features with a fluffy model of this type do, however, provide the high relative abundances of small grains measured *in situ* (Section 2.5).

Insight into the density of the cometary dust grains should be available from knowledge of the relative number of projectile and target ions that result from hypervelocity impacts (Ag is the target of PIA and PUMA—Figure 7). Most recent calibration studies based on the PUMA-1 instrument (Maas *et al.*, 1989) indicate silicate-dominated grains

have densities clustering around 2.5 g-cm^{-3} , whilst CHON-dominated grains appear to be fluffier, with mean densities of 1 g-cm^{-3} . Many of the smallest particles detected by PUMA were found to be silicates, implying that these are rather compact in nature.

1.4. COMPARISON AND CONSENSUS OF THE HALLEY DUST COMA FROM FLUENCES

Results from the various instruments and their individual calibrations (Section 1.2) can be combined into a coherent consensus on the dust fluxes and can be incorporated as a first step to compare the 'average' dust distributions measured on the three spacecraft encounters, namely the fluences. Such comparisons will have the best immunity to uncertainties of the nucleus orientation, its state of activity, and the vagaries of how its jets may intersect the three different spacecraft trajectories. We must, however, accept the task of *understanding* these differences, the yet unlocked mysteries due to the uncertain rotation state of comet Halley (Belton, 1989). A full comparison requires decoding of the jet structure, as we will see (Section 1.6), and is not yet resolved in terms of a proper rotation model for the nucleus.

Fluences (equal to the time integral of the flux, including missing data) are normalized first by reference to the miss distances of the three spacecraft. Scaling of flux according to an inverse square dependence on the cometocentric distance is quite appropriate for the fluence, although, of course, the deviations from this along different parts of the trajectory yield valuable information on the anisotropies of source emission and on the subsequent dynamic forces determining their trajectory prior to detection.

The resulting three fluence curves, shown in Figure 8, display the very different dust scenes encountered by the spacecraft. Although little variation in the number density of small particles ($< 10^{-16} \text{ kg}$) was experienced during the eight-day period, a decrease by a factor of as much as 30 was observed for typical micrometer-sized particles, a signature of not just heliocentric distance dependence, but also nucleus activity and perhaps the temporally changing nature of the source mass distribution.

Comparison of the fluences with a fountain model largely affected by heliocentric distance variations is also given in Figure 8. The model is based on that of Divine (1981), with extensions by Pankiewicz (1989a), and does show the importance of nucleus activity and coma dynamics over a simple dust production rate change.

The fluences particularly show the variation of the cumulative mass distribution index, α , over both mass and time (α is the gradient of the mass vs. cumulative flux curve in log-log space). Although model values typically have $\alpha = 0.88$ from 10^{-13} to 10^{-9} kg in the coma, measured values range from 0.75 ± 0.07 for VEGA 2 to 1.03 ± 0.15 for Giotto. The big surprise was that the large particle mass distribution ($> 10^{-9} \text{ kg}$), measured by DIDSY's large area acoustic sensors, recorded a remarkably flatter distribution, with $\alpha = 0.55 \pm 0.20$ (Figure 9). This has more recently been evidenced further by changes in Giotto's spin axis observed from oscillations in the field of view of the Halley Multicolour Camera (HMC) deduced from the effect of large particles that struck the spacecraft (Curd and Keller, 1988) very near to closest approach.

Giotto's 600-km flyby certainly appears to have been made at a fortuitous time, when absolute production rates for micrometer-sized particles were at least a factor of 3 below their expected values.

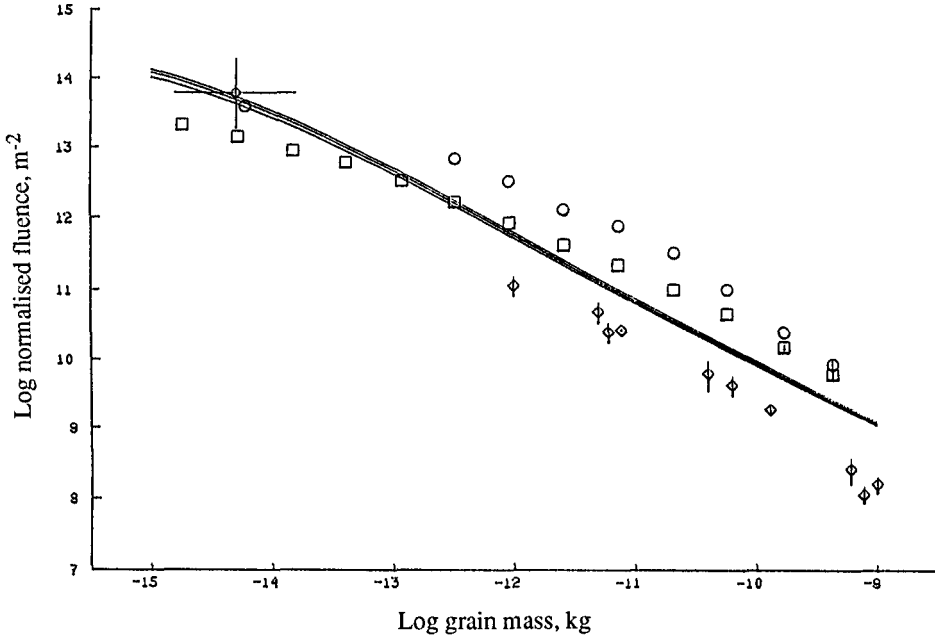


Figure 8. Fluences measured in Halley's coma are normalized by the varying closest approach distances for the VEGA 1 (circles), VEGA 2 (squares) and Giotto flybys (diamonds) to produce an average intercomparison over the mass range of 10^{-15} to 10^{-9} kg. Solid lines indicate fountain model distributions, decreasing in absolute values over the 8-day interval by a factor of only 0.8.

1.5. MASS AND AREA DISTRIBUTIONS AS PROPERTIES OF THE MEASURED DUST FLUXES

Mass and area distributions provide a most useful derivative of the measured fluence, indicating, for example, the material available to absorb and scatter the light detected remotely in ground-based observations. Whilst the area distribution is weighted (relative to the original fluence) by the square of the grain radius s^2 , the mass distribution must be weighted as $r(s) \cdot s^3$, thereby introducing the density distribution $r(s)$. A change of slope in the measured fluence will therefore affect area and mass distributions significantly and differently. A cumulative mass distribution index of $\alpha < 0.67$ will result in an increasing area distribution for the larger particles. To produce the same trend in the mass distribution, it is required that $\alpha < 1.0$ with a *constant* density function. Most density distributions are expected to be only weakly mass-dependent, however.

Figure 10 shows these derivatives for the Giotto fluence. A pre-Halley density model (Divine *et al.*, 1986) has been used to obtain the mass distribution, with

$$\rho = 3.0 - 2.2 \left(\frac{s}{s + s_0} \right) \quad (\text{g cm}^{-3}) \quad (1)$$

which does closely concur with determined densities in the range 1.0 to 2.5 g·cm⁻³ with s₀ = 2 μm (Section 1.3). Of particular interest to ground-based observers are the two peaks of the area distribution, at ~ 2 μm and ~ 2 mm. This function has further been used to compute the total cross-sectional area intercepted by Giotto with respect to cometocentric

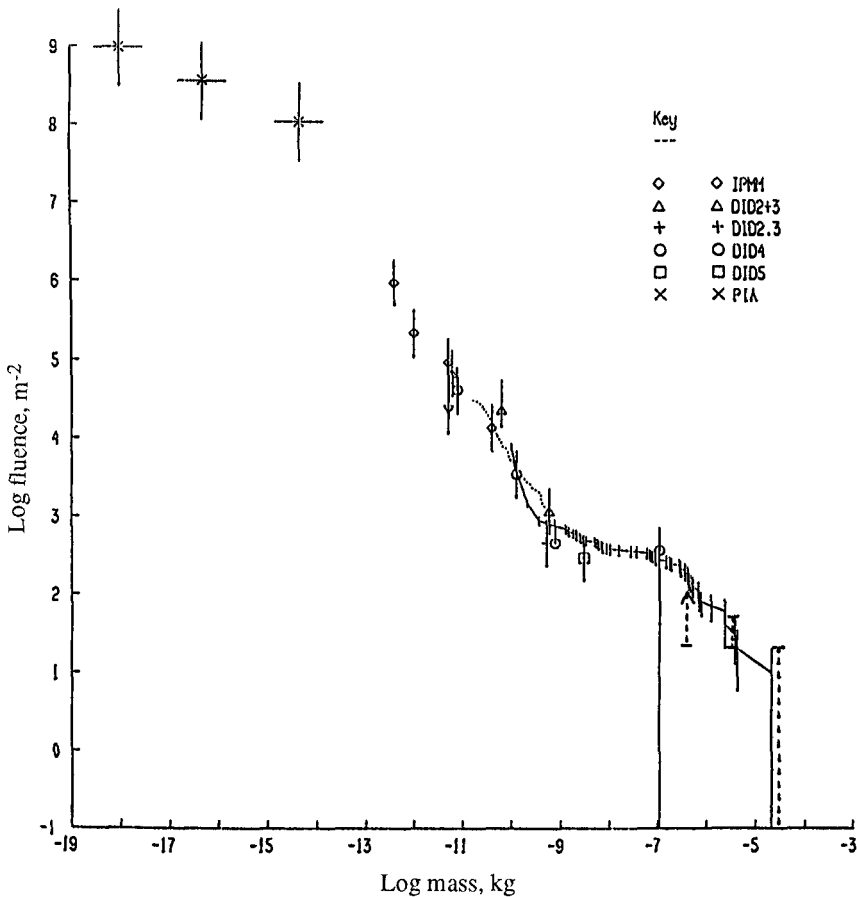


Figure 9. The complete PIA and DIDSY fluence (unnormalized) is shown in the full mass range from 10⁻¹⁹ to 10⁻⁵ kg (McDonnell *et al.*, 1989b). Uncertainties relating to momentum derating by penetrating impacts and counting statistics are given for the discrete fluence. Estimated fluences from the large particles recorded by the HMC are shown as three dashed lines to represent uncertainties (Curdt and Keller, 1989).

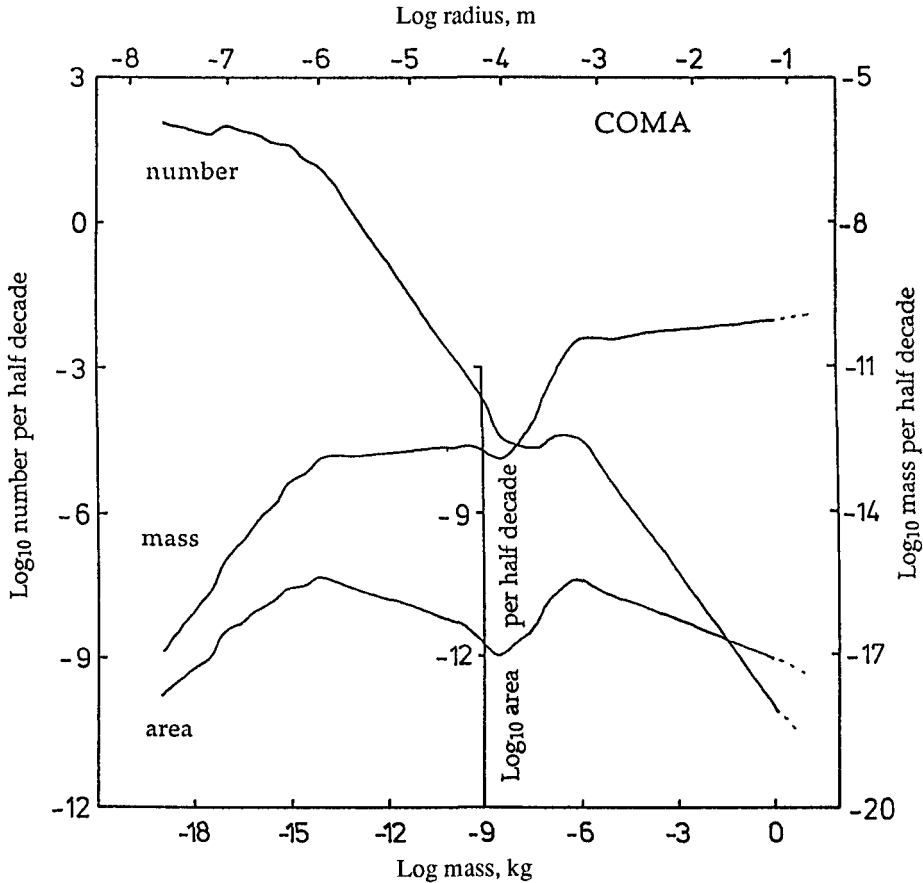


Figure 10. Number, area and mass distributions per cubic meter in the coma are shown, normalized to a distance of 600 km, derived from the Giotto PIA and DIDSY total fluence (McDonnell *et al.*, 1989b).

distance; the result derived from the measured *impact* fluence over a 7,000-km region has a radial (power law distance) gradient of -2.5 ± 0.1 (Nappo *et al.*, 1989). This has been directly compared by the same authors with the radial gradient from the Giotto optical probe experiment (HOPE), which recorded a radial gradient over the same region of -2.6 ± 0.1 , but the *in situ* data show uniquely that the scattering in this region is dominated by millimeter-sized grains.

1.6. DYNAMICS OF PARTICULATES WITHIN THE DUST COMA

Once dust grains have been accelerated from the sublimating cometary surface by gas pressure, their journey into the coma and on will involve, to the largest extent, radiation pressure and solar gravity as modifying forces. What the *in situ* study of impacting grains has shown is that our knowledge of these effects on intermediate-sized grains is fairly accurate; however, abundances of small ($< 10^{-19}$ kg) and large ($> 10^{-9}$ kg) grains do show significant deviations. In describing the dynamics of the particles measured at Halley, it is convenient to split the coma into two regions corresponding to (i) gas-free flow far from the nucleus and (ii) near-surface dust acceleration.

1.6.1. *Outer Coma Dynamics.* The large measured abundances of small particles at nearly all cometocentric distances less than 250,000 km (Figure 11) is indicative of a gap in pre-encounter mass distribution or optical property modelling; this is not really surprising, however, due to the very low scattering cross-sections from which the models were derived (Divine and Newburn, 1987).

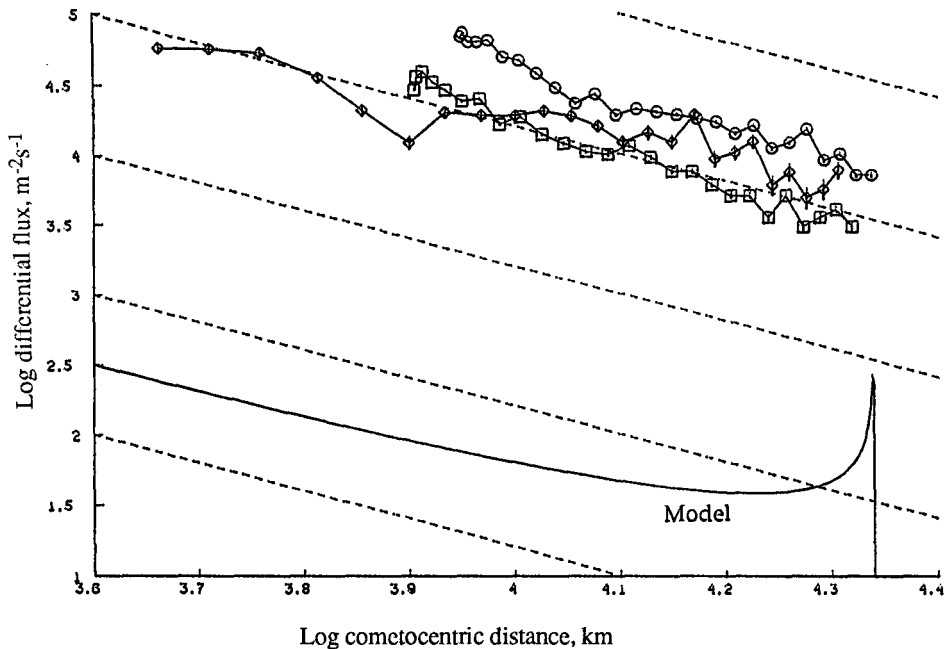


Figure 11. Differential fluxes in the mass range 6×10^{-18} to 6×10^{-17} kg for VEGA 1 (circles), VEGA 2 (squares) and Giotto PIA (diamonds). The solid curve is the model for Giotto only, as predictions for the VEGA flybys gave zero density (Pankiewicz, 1989). Dashes are inverse square comparisons.

Apex boundaries, expected from modelling to be drastic, were not as sharp as anticipated (Vaisberg *et al.*, 1987; McDonnell *et al.*, 1987). Changes in the radial slope that are apparent, however, are coincident with changes in mass distributions, indicating a much more diffuse effect of radiation pressure segregation (Divine *et al.*, 1986; Bertaux and Cot, 1983).

Closer in to the nucleus, but still at distances of 100,000 to 200,000 km, the DUCMA instrument on board both VEGA spacecraft detected non-Poissonian clustering of particles, described as 'dust packets' (Simpson *et al.*, 1987). This was later confirmed by studying large-distance, low-mass particle detections of the SP-1 experiment (Simpson *et al.*, 1989). The interpretation appears to be best argued by having large grains resembling conglomerates of small particles, gently disintegrating at varying distances throughout the coma. If conglomerate breakup is associated with major jets (Simpson *et al.*, 1987), the release of small particles, and presumably of trapped gas, might account for the apparent confinement of gases with a well-defined jet structure, such as the ground-based observations of CN jets (A'Hearn *et al.*, 1986).

At the larger particle end of the distribution, measured by Giotto DIDSY, the number of impacts is generally low, but the temporal distribution is significantly different on either side of closest approach (McDonnell *et al.*, 1987). The preponderance of large grains is to be found pre-encounter (Figure 6 and Figure 12) and can be interpreted in two differing ways, according to whether this behavior is peculiar to the encounter time of Giotto, or is typical of the coma average (Pankiewicz, 1989a).

The uniqueness of the large-particle data at Giotto's encounter is unfortunate from this point of view in testing these ideas, but because large-particle velocities in the coma are so low (typically much less than 100 m s^{-1} for those discussed here), it is hard to attribute high fluxes pre-encounter to varying source activity alone. More likely, and in fact predicted by Fertig and Schwehm (1984), is the changing effect of the solar gravity field on these large, low-velocity particles, causing increasing spatial density in the coma towards the comet's orbital motion, which was almost opposite to that of Giotto's trajectory. A problem to be tackled, though (but see Section 1.6.2), is that of the detection of these large particles in the last few minutes prior to closest approach, when Giotto was expected to be over the unilluminated side of the nucleus.

1.6.2. Near-Nucleus Dynamics. Although the most important region dynamically occurs at nuclear altitudes of less than 20 km, the spatial distribution measured by the encounter experiments can yield something about those effects when fine-resolution flux structure is compared, after accounting for grain trajectories, with emission sites determined from camera or ground-based observations.

Jet features appear to dominate the flux profiles of the near-nucleus coma, so that most of the dust is, in fact, expelled from relatively active regions on the sunlit surface into the sunward hemisphere (Keller *et al.*, 1986). To test this more carefully and deduce a map of the most active surface regions, the grain dynamics and nucleus rotation state are the factors most needed. The active surface regions could then be related to ground-based observations of jets, which can independently give the rotation state and hence the distribution of jet sources observed over a longer time period.

Reviews concerning Halley's nucleus rotation are presented elsewhere in this volume (Belton, *ibid.*), and rather than yielding a stable consensus, they provide the reader with some indication of the lack of harmony from the various sources. Estimates of the

rotation state from using dispersion in impact data appear to be no exception (Pankiewicz *et al.*, 1989a), although PIA and DIDSY data do accommodate periods of 36, 95 and 156 hours, which loosely correlate to the contemporary values of 52, 89 and 178 hours (Belton, 1989).

Non-radial acceleration in the early stages of outflow may result in such confusion (certainly in the dust impact data). Other possible sources of confusion might include the relationship between solar illumination and nucleus shape (Pankiewicz *et al.*, 1989b), surface breezes close to the nucleus, affecting the observed distribution of dust just above the surface (Keller and Thomas, 1989), and significant nucleus precession invoking a more complex jet pattern than expected (Watanabe, 1989).

1.7. INFERRED PROPERTIES OF NUCLEUS EMISSION

To a certain extent, the relative dust emission from Halley's nucleus has been discussed from the dynamical viewpoint in Section 1.6.2. Further remaining questions, how-

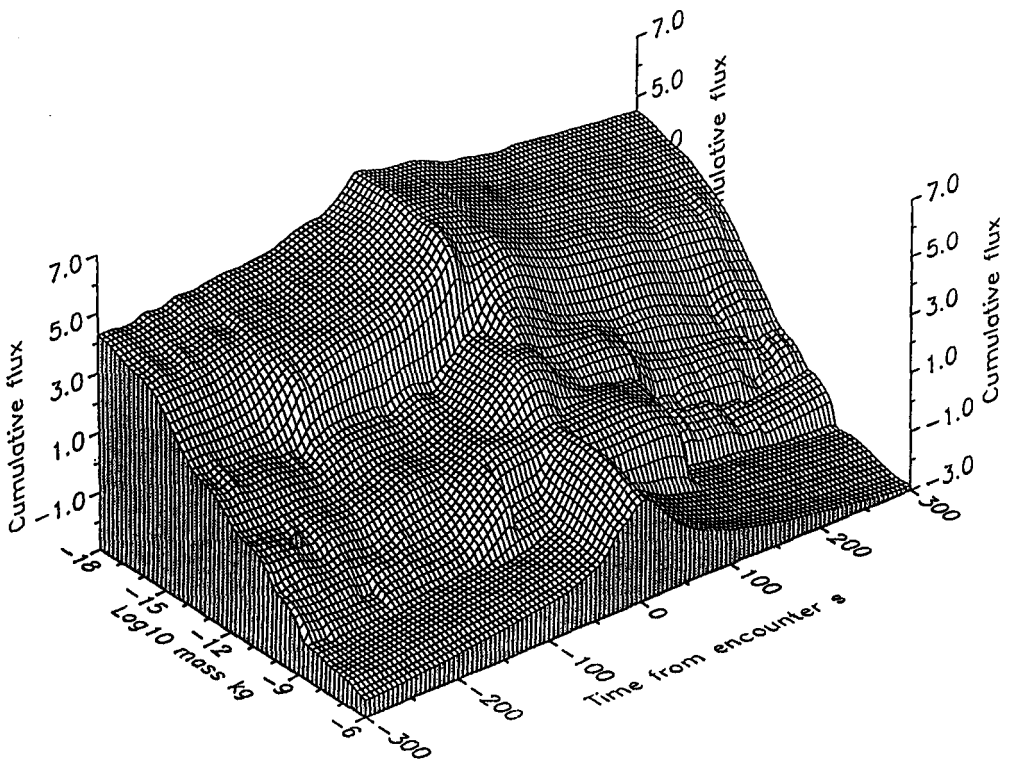


Figure 12. A three-dimensional representation of cumulative fluxes from 10^{-18} to 10^{-6} kg measured by Giotto DIDSY and PIA over a nucleus range of 20,500 to 600 km.

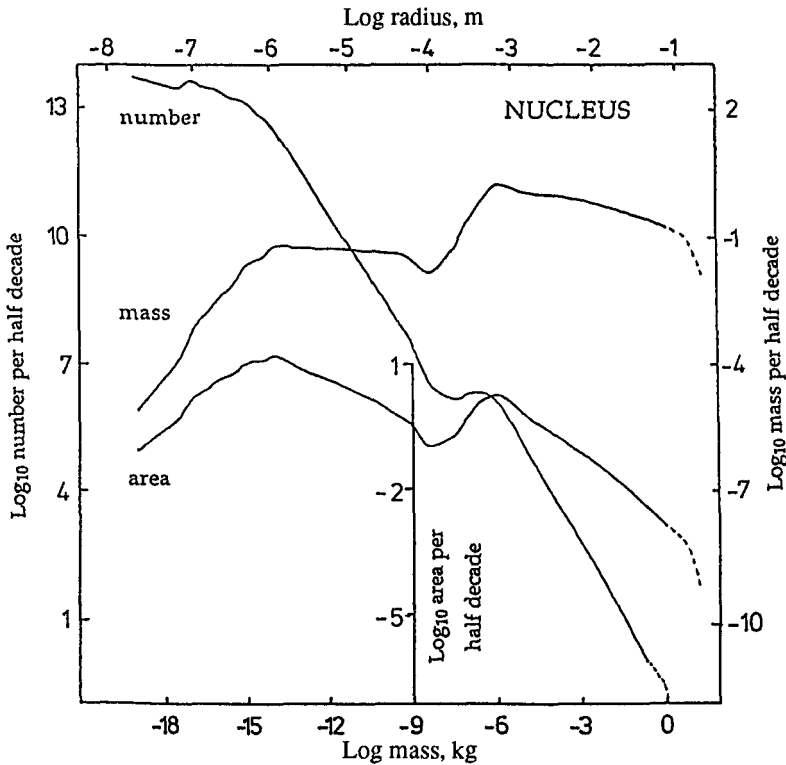


Figure 13. Number, area and mass distributions at the nucleus have been derived by using inverse square scaling and a semi-empirical dust velocity (Divine, 1981), from the total fluence measured by Giotto PIA and DIDSY (McDonnell *et al.*, 1989b).

ever, involve the mass distribution at the nucleus surface (what does a comet production surface *look like?*), and the global dust-to-gas mass ratio inferred from the *in situ* observations.

By scaling the coma fluence for the dust velocity distribution (Divine, 1981) and using simple inverse square cometocentric distance dependence (Section 1.4), the nucleus surface flux rate can be calculated. Figure 13 gives the number, mass and area distributions obtained in this way, incorporating a maximum liftable grain mass of 10 kg. This is of concern in deducing the dust-to-gas mass ratio, as it will depend on the largest grain size present in the nucleus, which may be larger or *smaller* than this value of maximum liftable mass.

If the measured gas production rate of $2.55 \times 10^4 \text{ kg}\cdot\text{s}^{-1}$ (Krankowsky *et al.*, 1986) at the time of the Giotto encounter is compared with the derived source flux, the dust-to-gas mass ratio can be obtained as a function of mass. The observed fluence extrapolated up to the largest liftable mass yields a ratio ~ 3 (Figure 14). The largest particles

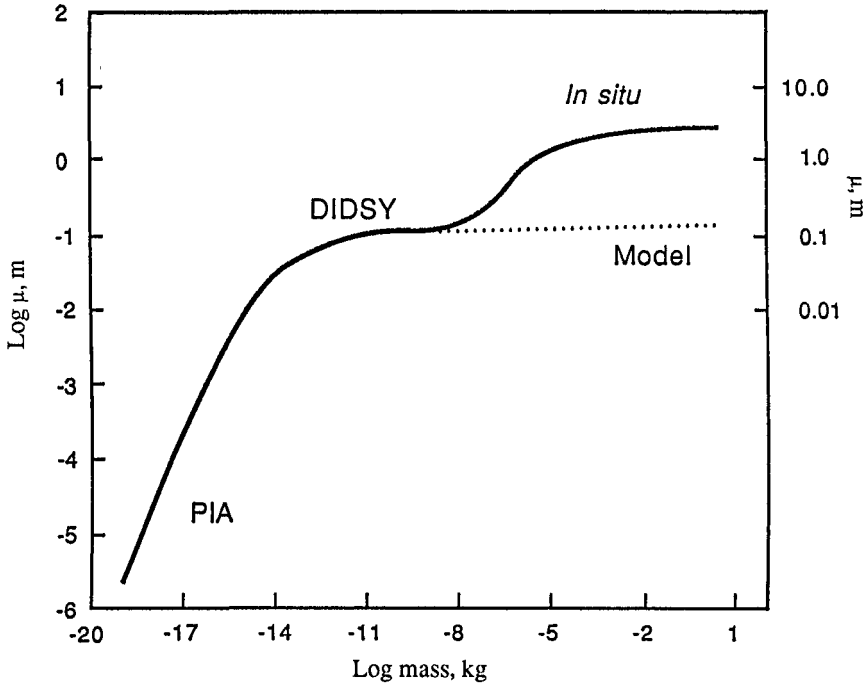


Figure 14. The dust-to-gas mass ratio is shown as a function of the largest grain present. The model curve signifies the ratios that would be obtained for a constant mass distribution index α at large masses, used, for example, by Divine *et al.* (1986). Limits to the value for Giotto's encounter with Halley are 1.3 (the largest *measured* mass) and 3 (the maximum liftable grain mass); a compromise of 2 is suggested.

measured by DIDSY of $\sim 10^{-5}$ kg indicate a lower limit of 1.3 if the observed mass excess in the coma is representative of the average.

There is now considerable evidence for abundances of millimeter- to centimeter-sized grains in cometary comae (Eaton *et al.*, 1984; Campbell *et al.*, 1989; Fulle *et al.*, 1988), so that emphasis on a dust-to-gas mass ratio of 2 for Halley during Giotto's encounter must be given (McDonnell *et al.*, 1989c). Comparison with VEGA distributions will place this value in context with respect to the epoch of measurement, especially since ground-based infrared observations of silicate emission (Hanner *et al.*, 1987) are inclined to show that, for much of the time, grains of less than 20- μm size dominate the coma.

2. Properties Deduced From Optical Measurements

2.1. INTRODUCTION

The question we now wish to address is the information on the physical properties of cometary dust that may be inferred from optical measurements. By these measurements

we specifically mean the reflected solar light off the cometary grains; thermal emission is addressed in a separate review, although we do consider the 3.4- and 9.7- μm infrared emission features in Section 2.5 with their chemical and morphological implications.

Reflected brightness measurements consist of either total or polarized light in various bandpasses from the ultraviolet to the near-infrared. A convenient way to present and discuss these measurements is to deduce the color and the polarization of the scattered light as a function of wavelength and scattering (or phase) angle. How the measurements relate to the physical properties of the dust is certainly a difficult question. In a very basic approach, they relate to the optical properties (i.e., complex index of refraction), and therefore to composition, to the texture or surface aspect and to the size, or size distribution of the grains. It is well-known that the interplay of the properties preclude any unambiguous determination and that one should really look for a broad characterization or a range of properties that satisfy the observations.

Since the publication of a review by one of us (Lamy, 1985), a considerable amount of observational data has been obtained. An overall synthesis is beyond the scope of the present article and we only address several aspects that raise new questions, reveal the complex nature of cometary dust and challenge the interpretation. We emphasize that this situation calls for increased rigor in the definition of physical parameters and in the procedures used to derive them: several of them are critically evaluated and sometimes rejected.

2.2. THE COLOR OF COMETARY GRAINS

2.2.1. Observational Results. The color is best studied using the reflectivity $S(\lambda)$ and the normalized reflectivity gradient $S'(\lambda_1, \lambda_2)$ following Jewitt and Meech (1986a). These authors have observed a common average behavior for both S and S' for a dozen comets: a strong reddening in the ultraviolet gradually leveling off as the wavelength increases, with the color becoming neutral at $\lambda = 2 \mu\text{m}$ and blue beyond $3 \mu\text{m}$, approximately. Lamy *et al.* (1989a) have regrouped observational results for Halley and shown that it follows this average law very well (Figure 15) and further that its color properties do not appear to change significantly between pre- and post-perihelion times.

This 'universal' behavior may, however, be limited and further mask a more complex reality. Indeed, Jewitt and Luu (1989) have recently reported that the dust coma of P/Tempel 2 has a neutral color. But perhaps even more interesting are the spatially resolved color observations that have been obtained for Halley:

- (i) A gradient in the J-H and H-K colors within 8,000 km of the nucleus was found in November 1985, with the bluest color at the photocenter (Campins *et al.*, 1989).
- (ii) Spatial structures in the color were observed when blue and red Charge Coupled Device (CCD) images were ratioed in March 1986. Hoban *et al.* (1989) found dust envelopes redder than the surrounding dust coma with a strong jet even redder. Lamy *et al.* (1989a) observed a strong asymmetry between the solar and anti-solar hemisphere, with the former being redder than the latter; a similar trend, in which the coma became redder with increasing distance in the sunward direction, was observed in April 1986 by Jewitt and Meech (1986b) from spectrophotometric observations.

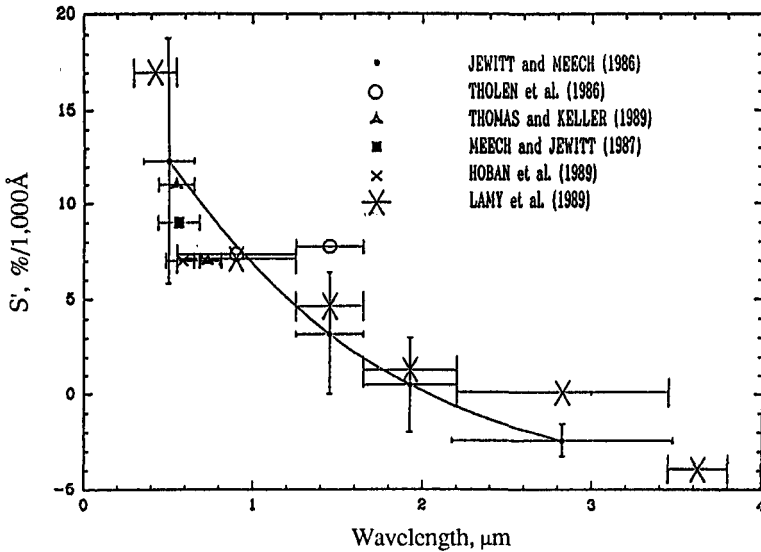


Figure 15. The normalized reflectivity gradient (S) for comet Halley is shown as derived by a number of authors, showing strong reddening at ultraviolet wavelengths (Lamy *et al.*, 1989b).

- (iii) Azimuthal variations of the color obtained with the Giotto HMC (Thomas and Keller, 1989) showed a lower reddening in the anti-solar direction.
- (iv) *In situ* optical probing by the Giotto HOPE photopolarimeter indicated that the color changed from red to neutral as the spacecraft approached the nucleus.
- (v) A neutral color from 0.3 to 1.7 μm was observed by the VEGA 2 TKS spectrometer after averaging over phase angles between 14° and 110° .

The interpretation of these data represents a formidable task. Here we limit ourselves to general considerations aimed at stimulating further research.

2.2.2. General Considerations About the Color. As extensively discussed by Perrin and Lamy (1989) for the case of the zodiacal light, the color of a dust cloud is determined by the interplay of various physical parameters in a complex way. Let us only mention these parameters appropriate to the cometary case (fixed scattering angles), i.e., those that do not involve the integration over the scattering angle along the line of sight as is the case for the zodiacal light:

- (i) The composition influences the color via the complex index of refraction $n(\lambda)$. The composition's influence on the color is particularly strong in the ultraviolet because of the rapid variation of $n(\lambda)$.
- (ii) The influence of the size distribution, as pointed out by Perrin and Lamy (1989), is convolved with the spectral variation of the imaginary part k of $n(\lambda)$. In particular, if k increases as λ decreases, any blue effect predicted

in the pure Rayleigh regime is counterbalanced (this was found to be the case for an organic material). In fact, the simple Rayleigh behavior (that, in the presence of large quantities of small particles, leads to a blue color), is never obeyed by 'real' grains.

- (iii) The roughness of the grains has a moderate influence on the color, which depends upon its scale with respect to the interacting wavelength; a small-scale roughness leads to a red color, and a large-scale one to a blue color (see also Schiffer, 1985).

The very comparison of observational color results with theoretical models raises problems that are usually not fully realized. The observations yield the color of the volume scattering function $\psi(\theta, \lambda)$, i.e., the phase function of a unit volume of the dust cloud (that is integrated over the size distribution), which involves differential cross-sections. Model calculations such as those performed by Jewitt and Meech (1986) or Hoban *et al.* (1989) are based on the total scattering cross-sections (also averaged over the size distribution). There is strictly no relationship between differential and total cross-sections, but, furthermore, experimental studies have shown that the shape of the phase function or $\psi(\theta)$ varies with wavelength (Killinger, 1987). It is therefore imperative that the model calculations should be performed with the differential cross-sections at the proper scattering angle. Note that cometary comae have dimensions such that the variation in scattering angle is minute and may be neglected. However, the effect of the phase function must be accounted for if observations taken at different dates (different scattering angles) are to be compared.

2.2.3. Interpreting Cometary Results: A First Approach. The gross variation of the reflectivity or its gradient with wavelength is probably controlled, to a large extent, by the optical properties of the grains, i.e., their composition. The calculations performed so far on various materials indicate that chondritic grains exhibit a color trend (Figure 16) in agreement with observations (Lamy and Perrin, 1986), in particular, the strong variation in the ultraviolet as emphasized by Roettger *et al.* (1989). This is very consistent with the fact that the optically dominating particles, which lie in the size range of 1 to 100 μm , have a composition close to that of the primitive meteorites.

The spatial variations of the color pose a more difficult problem, and the respective influence of size and composition may be difficult to disentangle. The dynamical evolution as determined by gas drag and radiation pressure leads to the well-known spatial segregation of the coma grains (Section 1.6). Fragmentation is also a possible explanation for color variations (Section 1.6.1). So far, there have been few interpretations limited to one particular observational result. Jewitt and Meech (1986a) found that size sorting by radiation pressure is able to explain the color gradient in the solar direction, an interpretation disputed by Hoban *et al.* (1989), who claim that all the points measured were outside the dust paraboloid. However, they find this mechanism adequate to explain their own observation of redness of the envelopes and jets, as it leads to an apparent excess of intermediate-size particles (typically 0.5 to 0.9 μm).

Lamy *et al.* (1989a) have emphasized that the solar/anti-solar asymmetry of the color is a consequence of the strong difference of the geometry of the inner coma in the blue ('circular' isophotes) and in the red (reinforced solar hemisphere). It is conceivable that the small grains experience a more isotropic outflow than the larger ones, but it is rather unclear that the small grains' contribution to the observed brightness can indeed influence the color.

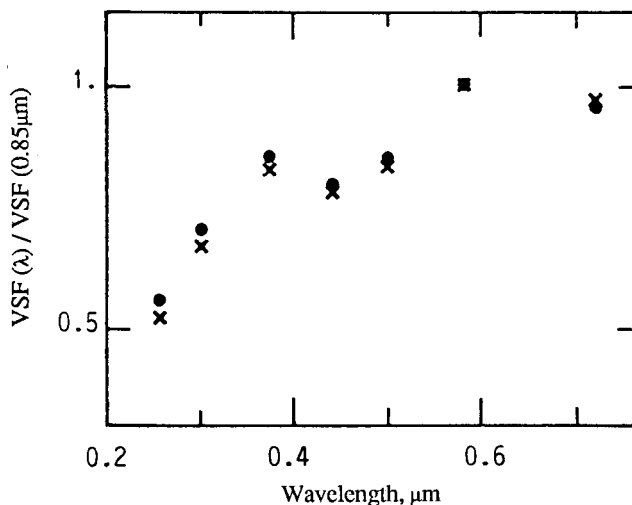


Figure 16. The variation of the volume scattering function $\psi(\theta, \lambda)$ is shown as a function of optical wavelength for chondritic grains.

2.3. THE POLARIZATION OF COMETARY GRAINS

2.3.1. Observational Results. Reviews of the measurements of polarization in comets have been presented by Dobrovolsky *et al.* (1986) and Lamy (1985). Perrin and Lamy (1987) have performed a critical evaluation of the data on 10 comets and concluded that, while there was no universal cometary polarization curve, the negative branch of polarization in the backscattering domain is an outstanding feature present in all observed comets. Dollfus *et al.* (1988) have produced a synthesis of the measurements obtained with diaphragm photopolarimetry on Halley that well-characterizes the various aspects of the polarization (Figure 17). Unfortunately, this type of measurement gives only a slight idea of the most important properties discovered on comet Halley, namely the enormous spatial and temporal variations. We now concentrate on this aspect, which is best revealed by two-dimensional polarization maps reconstructed from polarized CCD images. Eaton *et al.* (1988) obtained such data on December 13, 1985, and January 5 and 7, 1986, which indicate that the level of polarization is strongly correlated with the activity of the nucleus and the presence of jets as the latter exhibit increased polarization over the surrounding coma: on January 7, the polarization reached 18.4%, some 7% above the value from the 'average' polarization curve! Polarization maps from March 13 to 18, 1986 (Lamy *et al.*, 1989b), confirm these dramatic spatial and temporal variations correlated with jet activity and superimposed on a general solar/anti-solar asymmetry. The infrared polarization map at 2.2 μm obtained by Pankiewicz (1989b) on December 7, 1985, also reveals this asymmetry, with the maximum of polarization in the anti-solar region. In fact, as noted by Eaton *et al.* (1988), polarized images are very good probes of nuclear activity. This leads to questioning the validity of a single polarization curve for active comets.

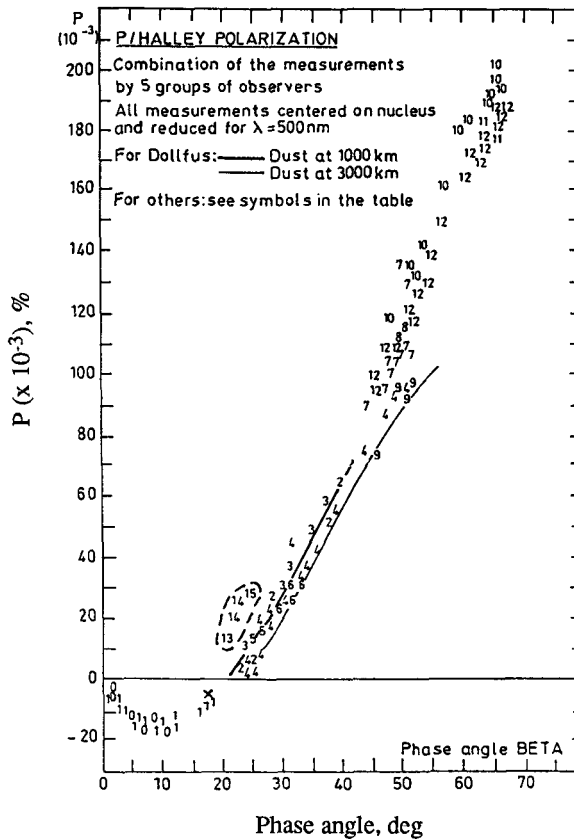


Figure 17. Photopolarimetric measurements near comet Halley's nucleus were taken by five groups of observers (from Dollfus *et al.*, 1988). Numbers indicate the dates of observation, with outliers 13, 14 and 15 being noted.

2.3.2. *General Considerations on the Polarization.* The polarization of a dust cloud is determined by the same physical parameters as for the color, but in a different way. Although not extensive, the investigation by Perrin and Lamy (1987) allows us to point out that:

- (i) The value of maximum polarization (and its corresponding scattering angle) is mostly controlled by the imaginary part of the refractive index.
- (ii) The grain roughness has a very strong influence on the polarization curve.

As a consequence, the application of the Mie theory valid for perfect spheres becomes extremely questionable, if not meaningless, for the interpretation of the polarization of cometary grains.

2.3.3. *Interpretation.* Owing to the above remark, it is not surprising that attempts to reproduce cometary polarization curves using the Mie theory have largely failed, as illustrated by the systematic investigation performed by Myers and Nordsieck (1984) for comets Churyumov-Gerasimenko and Austin. Mukai *et al.* (1987) have attempted to retrieve the complex refractive index from Mie scattering modelling of the polarization curve of comet Halley (particularly its negative branch) using the size distribution obtained by the VEGA spacecraft. Perrin and Lamy (1987) have already emphasized the instability of the solution with respect to both the refractive index (constrained to an unrealistically narrow range) and the size spectrum, and concluded that the negative branch is naturally and best explained by the presence of large, rough grains. Indeed, Lamy *et al.* (1987) have obtained a satisfactory fit to the average polarization curve of comet Halley using a model for light scattering by rough particles (Figure 18); this is consistent with the fact that grains larger than a few micrometers contribute the most to the total brightness of the coma.

The spatial and temporal variations in the polarization have only been addressed in general terms by Eaton *et al.* (1988): the increase of polarization in the jets may be a result of different size distribution, different composition of grains or both. In fact, the variations are so important that, coupled with color effects, they should allow the characterization of the properties of jet dust particles in comparison with 'background' particles.

2.4. THE ALBEDO OF COMETARY GRAINS

The albedo is a convenient parameter that characterizes how efficiently a given grain scatters light, i.e., in simple words, if the grain is mostly white, grey or black.

It was only with the work of Hanner *et al.* (1981) that the definition of the various albedos was clarified and that the geometric albedo $A_p(\theta)$ most appropriate to dust particles was introduced. $A_p(\theta)$ is referred to a white Lambertian disc of the same geometric cross-section G .

$$A_p(\theta) = \frac{\pi}{G \sigma(\theta)} \quad (2)$$

This definition involves the differential scattering cross-section $\sigma(\theta)$ at scattering angle θ , consistent with the quantities being observed as pointed out for the color. This geometric albedo may either be computed, using, for instance, the Mie theory, or measured on isolated dust grains (Giese *et al.*, 1986; Killinger, 1987).

The determination of the albedo of cometary grains immediately raises problems, since the observations of the scattered intensity only yields the volume scattering function $\psi(\theta, \lambda)$, i.e., the phase function averaged over the size distribution function. Deriving an 'averaged' albedo has no real meaning, since the broadness of the size spectrum implies that very different scattering regimes are present. Indeed, two independent lines of evidence show that the geometric albedo is a function of grain size:

- (i) Laboratory measurements by Giese *et al.* (1986). As an example, $A_p(180^\circ)$ for an absorbing material decreases from 0.1 for a grain radius of 2 μm to 0.02 for a radius of 60 μm .
- (ii) Model calculations. Lamy *et al.* (1987) have computed geometric albedos $A_p(107^\circ)$ averaged in narrow size intervals ($\Delta s/s = 0.1$) to smooth out any

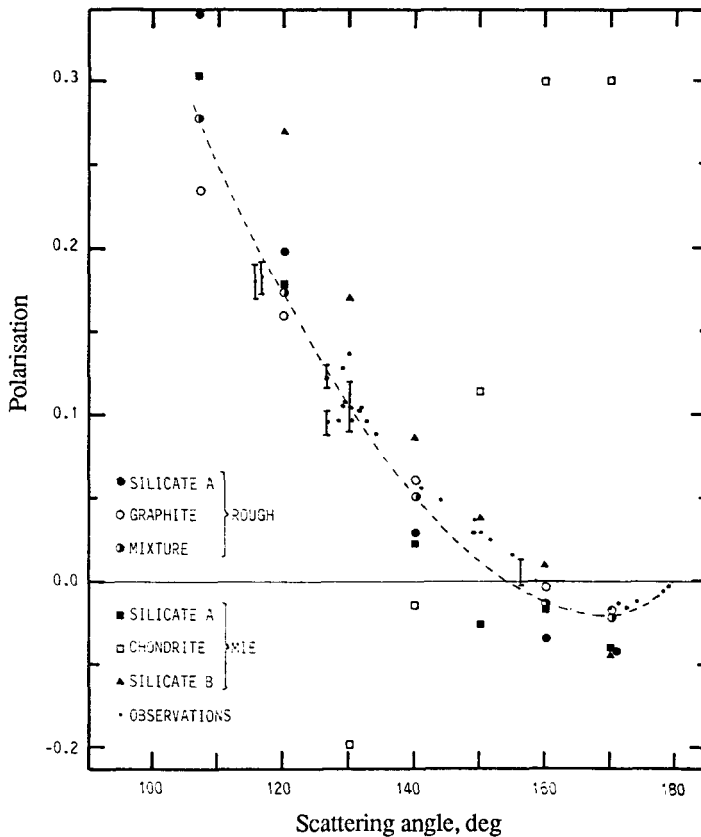


Figure 18. Fits to the polarization curve of comet Halley (at large scattering angles) are shown for a variety of grain types (from Lamy *et al.*, 1987). Rough particles (circles) produce the best comparison with observation (dots).

resonance while preserving the same scattering regime; they found the same trend for a silicate material with $A_p = 0.035$ for a radius of $1 \mu\text{m}$ and $A_p = 0.02$ for a radius of $10 \mu\text{m}$.

Two methods have been proposed so far to derive the albedo from the observations. Both are derived from the study of large bodies (satellites, asteroids) and look highly suspect, since their formal application to dust particles has never been established. They further yield an 'averaged' albedo whose physical meaning has been questioned above.

The combination of visible and infrared photometries supposedly gives access to the albedo $A = Q_{\text{sca}}/Q_{\text{ext}}$. However, the derivation given by O'Dell (1971) applies only to a single particle (not a size distribution) and makes totally unrealistic assumptions (e.g., the dependence of the scattering function upon the scattering angle is disregarded). In fact, it

can be shown that it is generally impossible to retrieve the geometric albedo $A_p(\theta)$ of cometary grains by this method (Lamy and Perrin, in preparation).

The use of the polarization curve to derive the albedo is based on an empirical law relating the polarimetric slope h (at the point of polarization inversion) to the surface normal reflectance established from laboratory measurements on pulverized minerals (Veveřka and Noland, 1973). For a planet, this reflectance is the ratio of planet brightness at zero phase angle to the brightness of a perfectly diffusing disc with the same position and apparent size, that is, its geometric albedo p (Allen, 1973). That this empirical law applies as well to dust particles and is able to yield $A_p(180^\circ)$ has never been proven or even tested. A blind application has already been questioned by Perrin and Lamy (1987), who further noticed that the saturation effect (i.e., a maximum value of h of 0.003 deg^{-1}) appears to be ignored by dust grains. Indeed, laboratory measurements by Killinger (1987) reveal that irregular particles may exhibit h values as large as 0.008 deg^{-1} , well outside the empirical law for pulverized materials. As a consequence, albedo values of cometary grains derived by this method (e.g., Dollfus, 1989) are highly suspect.

In view of this situation, the best indications for the albedo probably come from general consideration of light scattering by dust particles based on laboratory measurements and theoretical calculations. As seen in Section 2.3, the polarization curve calls for the presence of large, rather absorbing, rough grains, which necessarily have a rather low albedo (Giese *et al.*, 1986): a range of values of $A_p(180^\circ)$ of 0.02 to 0.1 is what really can be given safely.

2.5. THE 3.4- μm AND 9.7- μm INFRARED EMISSION FEATURES

Greenberg has considered in detail the 3.4- μm and 9.7- μm *excess* emission of cometary dust above the continuum, which could provide a strict set of constraints on both the chemical and morphological properties of the dust.

The chemistry is, at least qualitatively, determined from the 3.4- μm emission, which is attributable to CH absorption stretches in organic molecules, and the 9.7- μm emission, attributable to the SiO stretch in silicates. The fact that the silicate emission band shape is just about as narrow as the interstellar absorption feature dictates that the particles responsible for the 9.7- μm emission are less than $\sim 1 \mu\text{m}$ in size and thus are much smaller than those larger ones responsible for the continuum emission (Hage and Greenberg, 1989; Greenberg *et al.*, 1989a, b). Furthermore, the larger ones may not contribute substantially to the excess emission (which would lead to a shape distortion), *even though* the size distribution is continuous (the particles are such that they act bimodally in terms of excess emissions). This is a result of these larger particles being very fluffy rather than compact.

Using the usual assumption of a spherically expanding flow of dust and gas in the coma, the 3.4- μm and 9.7- μm excess emissions, if limited to 1- μm -size compact particles, lead to a derived Giotto fluence between 10^4 and 10^5 times that observed up to this mass ($1 \mu\text{m} \approx 1.3 \times 10^{-14} \text{ kg}$) (McDonnell *et al.*, 1987, 1989a), if the particle temperature is about 320 K. Since silicate particles (even small ones) are not heated much above this temperature (Hanner, 1988), the organic component must be invoked as the source of dust heating. As mantles on silicate cores (a coating layer of differing chemical composition), the organic refractory absorption in the visual (Chlewicki and Greenberg, 1989) appears sufficient to heat the particles to above 450 K, if they are limited to submicrometer size. Even so, the required mass fluence is still orders of magnitude too large if the particles are

compact, and the organic mass about equal, in the mean, to silicate masses as constrained by the Giotto and VEGA mass absorption spectra (Kissel and Krueger, 1987).

However, if the comet dust consists of sufficiently fluffy aggregates of such sub-micrometer particles, the upper mass limit may be raised by a factor of ~ 1000 , because a very loose aggregate of small particles, if considered as an entity that acts like a *sum* of its components; even though its total mass is 'large,' its temperature and emissivity approach those of its basic units considered separately as the porosity approaches unity. The actual requirement of fluffiness is a porosity of $P = 0.97$ (Greenberg *et al.*, 1989b), bringing the fluence more or less in line with that presented by McDonnell *et al.* (1989a) (too high with respect to the values published earlier by McDonnell *et al.* (1987), but consistent with more recent revisions of flux). At such high porosities, there is a sudden sharp temperature reduction and a reduction in spectral emissivity efficiency with size, giving the desired bimodality in spectral emissivity with unit mass. This high porosity result furthermore is consistent with a comet nucleus porosity of 0.8 predicted by Greenberg (1986, 1987) when the volatiles (H_2O , etc.) are reincorporated in the comet dust in the proportion they had before evaporation (Greenberg, 1982).

3. The Cometary Particulate

In situ measurements of dust at comet Halley during March 1986 have established spatial densities over trajectory lengths of more than 500,000 km and over a period of 8 days; the data provide opportunity, by invoking dynamical consideration of trajectories, to characterize the nucleus surface emission pattern over that time.

A new wealth of information has been gained on particles at extreme ends of the size distribution, where scattering efficiencies are low, and remote measurements ineffective. Small grains ($< 0.1\text{-}\mu\text{m}$ size) are more abundant than previously estimated, with particles extending down to the molecular scale; large particles in the gram range were certainly more numerous during the Giotto encounter, and this evidence for large particles is supported also by other sources such as radar, polarization and detailed Finson-Probstein modelling.

Small- to medium-sized grains show a very rich carbon-based chemistry, perhaps a clue as to their origin and present state. The bulk density of the grains (with masses less than 10^{-15} kg) has been deduced from the PUMA and PIA measurements (Section 1.3). Both CHON ($1\text{ g}\cdot\text{cm}^{-3}$) and silicate ($2.5\text{ g}\cdot\text{cm}^{-3}$) grains may have the nominal density of their constituents, indicating a rather compact structure. The density of the heavier grains (masses larger than 10^{-15} kg) may only be inferred when converting masses to radii for optical model calculations: there are indications that their density is lower than that of the bulk material, suggesting a non-compact structure. Significant evidence for the evaporation of volatiles from grains, and probably fragmentation, has been presented.

Optical measurements allow some insight into the physical properties of those cometary grains that are optically active. For remote sensing, the size interval from 0.5 to 100 μm is probably dominant, but an exception (Section 1.5) could be the *in situ* optical data from the HOPE experiment, where the DIDSY fluxes strongly point to dominance by millimeter-sized grains.

A picture emerges of rough, irregular grains whose composition is consistent with chondritic meteorites and whose albedo is probably low (0.02 to 0.1). The roughness

(deduced from polarimetric measurements) has interesting consequences for their behavior in the infrared; their equilibrium temperature is higher than that of a black-body leading to an enhanced thermal emission, and their infrared emission bands (e.g., 10 μm) are less structured than those of spherical grains.

Intercomparison of *in situ* and remote data has provided momentum for investigations of jet dust-gas relationships (the CN jets and fragmentation discussed in Section 1.6.1), even towards nucleus rotation state and surface emission. The characterization of the cometary particulate from both remote measurements and *in situ* impact and spectrometer data has yielded some answers concerning the bulk structure and composition of particulates, but much evidence concerning the nature of the surface of the nucleus and its emission processes yet lies undecoded.

Acknowledgments

Appreciation is recorded to the Principal and Co-Investigators from numerous experiments on board VEGAs 1 and 2 and Giotto. Also to colleagues at the reviewers' institutes, especially C.H. Perry and R. Beard, in the preparation of this document.

References

- A'Hearn, M.F., Hoban, S., Birch, P.V., Bowers, C., Martin, R., and Klinglesmith, D.A., III, 1986, 'Cyanogen jets in comet Halley,' *Nature*, 324, p. 649.
- Allen, C.W., 1973, 'Astrophysical quantities,' 3rd edition, the Athlone press, London.
- Belton, M., 1989, 'Rotational properties of cometary nuclei,' this volume.
- Bertaux, J.L., and Cot, C., 1983, 'Segregation of cometary dust grains by differential radiation pressure,' in 'Cometary Exploration II,' Budapest, p. 113.
- Brownlee, D.E., 1988, 'The composition of dust particles in the environment of comet Halley,' submitted to 'Comet Halley 1986: World-wide investigations, results and interpretations,' Ellis Horwood Publishing Ltd., Chichester, in press.
- Campbell, D.B., Harmon, J.K., and Shapiro, I.I., 1989, 'Radar observations of comet Halley,' *Astrophys. J.*, 338, p. 1094.
- Campins, H., Rieke, M.J., and Rieke, G.H., 1989, 'An infrared color gradient in the inner coma of comet Halley,' *Icarus*, 78, p. 54.
- Chlewicki, G., and Greenberg, J.M., 1989, 'Interstellar circular polarisation and the dielectric nature of dust grains,' submitted to *Astrophys. J.*
- Curd, W., and Keller, H.U., 1988, 'Collisions with cometary dust recorded by the Giotto HMC camera,' *ESA Journal*, 12, p. 189.
- Delsemme, A.H., 1977, 'The origin of comets,' in 'Comets, Asteroids, Meteorites,' ed. A.H. Delsemme, Univ. of Toledo Press, Toledo, p. 3.
- Divine, N., 1981, 'Numerical models for Halley dust environments,' ESA SP-174, p. 25.
- Divine, N., Fechtig, H., Gombosi, T.I., Hanner, M.S., Keller, H.U., Larson, S.M., Mendis, D.A., Newburn, R.L., Jr., Reinhard, R., Sekanina, Z., and Yeomans, D.K., 1986, 'The comet Halley dust and gas environment,' *Space Sci. Rev.*, 43, p. 1.
- Divine, N., and Newburn, R.L., Jr., 1987, 'Modeling Halley before and after the encounters,' *Astron. Astrophys.*, 187, p. 867.

- Dobrovolsky, O.L., Kiselev, N.N., and Chernova, G.P., 1986, 'Polarisation of comets: A review,' *Earth, Moon, Planets*, 34, p. 189.
- Dollfus, A., 1989, 'Polarimetry of grains in the coma of comet P/Halley. II: Interpretation,' *Astron. Astrophys.*, 213, p. 469.
- Dollfus, A., Bastien, P., Le Borgne, J.-F., Levasseur-Regourd, A.C., and Mukai, T., 1988, 'Optical polarimetry of P/Halley: Synthesis of the measurements in the continuum,' *Astron. Astrophys.*, 206, p. 348.
- Eaton, N., Davies, J.K., and Green, S.F., 1984, 'The anomalous dust tail of comet P/Tempel 2,' *Mon. Not. R. Astr. Soc.*, 211, p. 15P.
- Eaton, N., Scarrott, S.M., and Warren-Smith R.F., 1988, 'Polarisation images of the inner regions of comet Halley,' *Icarus*, 76, p. 270.
- Fertig, J., and Schwehm, G.H., 1984, 'Dust environment models for comet P/Halley: Support for targeting of the Giotto S/C,' *Adv. Space Res.*, 4(9), p. 213.
- Fulle, M., Barbieri, C., and Cremonese, G., 1988, 'The dust tail of comet P/Halley from ground-based CCD images,' *Astron. Astrophys.*, 201, p. 362.
- Giese, R.H., Killinger, R.T., Kneissel, B., and Zerull, R.H., 1986, 'Albedo and colour of dust grains: Laboratory versus cometary results,' *ESA SP-250, Vol. II*, p. 53.
- Greenberg, J.M., 1986, 'Predicting that comet Halley is dark,' *Nature*, 321, p. 385.
- Greenberg, J.M., 1987, 'Comet Halley: A carrier of interstellar dust chemical evolution,' *Adv. Space Res.*, 7(5), p. 33.
- Greenberg, J.M., 1982, 'What are comets made of? A model based on interstellar dust,' in 'Comets,' ed. L. Wilkening, Univ. of Arizona Press, Tucson, p. 131.
- Greenberg, J.M., Zhao, N.S., and Hage, J., 1989a, 'The interstellar dust model of comet dust constrained by 3.4 μm and 10 μm emission,' *Adv. Space Res.*, 9(3), p. 3.
- Greenberg, J.M., Hage, J., and Zhao, N.S., 1989b, 'From interstellar dust to comet dust: A unification of observational constraints,' submitted to *Astrophys. J.*
- Hage, J., and Greenberg, J.M., 1989, 'Optics of fluffy particles,' submitted to *Astrophys. J.*
- Hanner, M.S., 1988, 'Grain optical properties,' *NASA Conf. Publ. 3004*, p. 22.
- Hanner, M.S., Giese, R.H., Weiss, K., and Zerull, R., 1981, 'On the definition of albedo and application to irregular particles,' *Astron. Astrophys.*, 104, p. 42.
- Hanner, M.S., Tokunaga, A.T., Golisch, W.F., Griep, D.M., and Kaminski, C.D., 1987, 'Infrared emission from P/Halley's dust coma during March 1986,' *Astron. Astrophys.*, 187, p. 653.
- Hoban, S., A'Hearn, M.F., Birch, P.V., and Martin, R., 1989, 'Spatial structures in the color of the dust coma of comet P/Halley,' *Icarus*, 79, p. 145.
- Igenbergs, E., and Kuczera, H., 1979, 'Micrometeoroid and dust simulation,' *ESA SP-153*, p. 109.
- Jessberger, E.K., Christoforidis, A., and Kissel, J., 1988, 'Aspects of major element composition of Halley dust,' *Nature*, 332, p. 691.
- Jewitt, D.C., and Meech, K.J., 1986a, 'Cometary grain scattering versus wavelength or what color is cometary dust,' *Astrophys. J.*, 310, p. 937.
- Jewitt, D.C., and Meech, K.J., 1986b, 'Scattering properties of cometary grains — Comet P/Halley,' *ESA SP-250, Vol. II*, p. 47.
- Jewitt, D.C., and Luu, J., 1989, 'A CCD portrait of comet P/Tempel 2,' submitted to *Astron. J.*

- Keller, H.U., Arpigny, C., Barbieri, C., Bonnet, R.M., Cazes, S., Coradini, M., Cosmovici, C.B., Delamere, W.A., Huebner, W.F., Hughes, D.W., Jamar, C., Malaise, D., Reitsema, H.J., Schmidt, H.U., Schmidt, W.K.H., Seige, P., Whipple, F.L., and Wilhelm, K., 1986, 'First Halley Multicolour Camera imaging results from Giotto,' *Nature*, 321, p. 320.
- Keller, H.U., and Thomas, N., 1989, 'Evidence for near-surface breezes on comet P/Halley,' submitted as a letter to *Astron. Astrophys.*
- Killinger, R.T., 1987, Doctoral dissertation, Bochum University, FRG.
- Kissel, J., 1986, 'The Giotto Particulate Impact Analyser,' *ESA SP-1077*, p. 67.
- Kissel, J., and Krueger, F.R., 1987, 'The organic component in dust from comet Halley as measured by the PUMA mass spectrometer on board VEGA 1,' *Nature*, 326, p. 755.
- Krankowsky, D., Lämmerzahl, P., Herrwerth, I., Woweries, J., Eberhardt, P., Dolder, U., Herrmann, U., Schultz, W., Berthelier, J.J., Illiano, J.M., Hodges, R.R., and Hoffman, J.H., 1986, 'In situ gas and ion measurements at comet Halley,' *Nature*, 321, p. 326.
- Lamy, P.L., 1985, 'Cometary dust: Observational evidences and properties,' in 'Asteroids, Comets, Meteors II,' eds. C.-I. Lagerkvist et al., Uppsala University, Uppsala, p. 373.
- Lamy, P.L., Grün, E., and Perrin, J.M., 1987, 'Comet P/Halley: Implications of the mass distribution function for the photopolarimetric properties of the dust coma,' *Astron. Astrophys.*, 187, p. 767.
- Lamy, P.L., and Perrin, J.M., 1986, 'Comet Halley: Implications of the impact measurements for the optical properties of the dust,' *ESA SP-250*, Vol. II, p. 65.
- Lamy, P.L., Malburet, P., Liebaria, A., and Koutchmy, S., 1989a, 'Comet P/Halley at a heliocentric distance of 2.6 A.U. preperihelion: Jet activity and properties of the dust coma,' submitted to *Astron. Astrophys.*
- Lamy, P.L., Cosmovici, C., and Schwarz, G., 1989b, 'High resolution polarisation and color map of comet P/Halley,' in preparation.
- Maas, D., Krueger, F.R., and Kissel, J., 1989, 'Mass-density and composition-distribution of Halley's dust obtained by PUMA data,' in 'Asteroids, Comets, Meteors III' eds. C.-I. Lagerkvist et al., Uppsala University, Uppsala, p. 389.
- Mazets, E.P., Sagdeev, R.Z., Aptekar, R.C., Golenetskii, S.V., Guryan, Yu.A., Dyachkov, A.V., Ilyinskii, V.N., Panov, V.N., Petrov, G.G., Savvin, A.V., Sokolov, I.A., Frederiks, D.D., Khavenson, N.G., Shapiro, V.D., and Schevchenko, V.I., 1987, 'Dust in comet P/Halley from VEGA observations,' *Astron. Astrophys.*, 187, p. 699.
- McDonnell, J.A.M., 1987, 'The Giotto Dust Impact Detector System,' *J. Phys. E.*, 20, p. 741.
- McDonnell, J.A.M., Alexander, W.M., Burton, W.M., Bussoletti, E., Evans, G.C., Evans, S.T., Firth, J.G., Grard, R.J.L., Green, S.F., Grün, E., Hanner, M.S., Hughes, D.W., Igenbergs, E., Kissel, J., Kuczera, H., Lindblad, B., Langevin, Y., Mandeville, J.-C., Nappo, S., Pankiewicz, G.S., Perry C.H., Schwehm G.H., Sekanina Z., Stevenson T.J., Turner R.F., Weishaupt, U., Wallis, M.K., and Zarnecki, J.C., 1987, 'The dust distribution within the inner coma of comet P/Halley 1982i: Encounter by Giotto's impact detectors,' *Astron. Astrophys.*, 187, p. 719.

- McDonnell, J.A.M., Green, S.F., Grün, E., Kissel, J., Nappo, S., Pankiewicz, G.S., and Perry, C.H., 1989a, 'In situ exploration of the dusty coma of comet P/Halley at Giotto's encounter: Flux rates and time profiles from 10^{-19} kg to 10^{-5} kg,' *Adv. Space Res.*, 9(3), p. 277.
- McDonnell, J.A.M., Green, S.F., Nappo, S., Pankiewicz, G.S., Perry, C.H., and Zarnecki, J.C., 1989b, 'Dust mass distributions: The perspective from Giotto's measurements at P/Halley,' presented at IAU Colloquium No. 116, Bamberg.
- McDonnell, J.A.M., Pankiewicz, G.S., Birchley, P.N.W., Green, S.F., and Perry, C.H., 1989c, 'The comet nucleus: Ice and dust morphological balances in a production surface of comet P/Halley,' submitted to *Proc. XXth Lunar and Planetary Science*.
- Meech, K.J., and Jewitt, D.C., 1987, 'Observations of comet P/Halley at minimum phase angle,' *Astron. Astrophys.*, 187, p. 585.
- Mukai, T., Mukai, S., and Kikuchi, S., 1987, 'Variation of grain properties at the dust outbursts,' *ESA SP-278*, p. 427.
- Myers, R.V., and Nordsieck, K.H., 1984, 'Spectropolarimetry of comets Austin and Churyumov-Gerasimenko,' *Icarus*, 58, p. 431.
- Nappo, S., McDonnell, J.A.M., Lvasseur-Regourd, A.C., Mandeville, J.-C., Soubeyran, A., and Zarnecki, J.C., 1989, 'Intercomparison of Giotto DIDSY/PIA and HOPE data,' in 'Asteroids, Comets, Meteors III,' eds. C.-I. Lagerkvist et al., Uppsala University, Uppsala, p. 397.
- O'Dell, C.R., 1971, 'Nature of particulate matter in comets as determined from infrared observations,' *Astrophys. J.*, 166, p. 675.
- Pankiewicz, G.S., 1989a, 'Dust environment modelling from encounters with comet P/Halley,' Ph.D. thesis, University of Kent at Canterbury, U.K.
- Pankiewicz, G.S., 1989b, 'Polarimetric observations of comets P/Halley and P/Giacobini-Zinner at $2.2\mu\text{m}$,' *Workshop on Polarisation of Light Scattered by Cometary Dust (II)*, Paris, France.
- Pankiewicz, G.S., McDonnell, J.A.M., and Perry, C.H., 1989a, 'In situ exploration of the dusty coma of comet P/Halley at Giotto's encounter: Nucleus emission and production rates from temporal variability,' *Adv. Space Res.*, 9(3), p. 273.
- Pankiewicz, G.S., Beard, R., Green, S.F., and McDonnell, J.A.M., 1989b, 'The rotation state of comet Halley from dust measurements: The search continues,' presented at IAU Colloquium No. 116, Bamberg.
- Perrin, J.M., and Lamy, P.L., 1987, 'Similarity and diversity of the polarisation of comets,' *ESA SP-278*, p. 411.
- Perrin, J.M., and Lamy, P.L., 1989, 'The color of the zodiacal light and the size distribution and composition of interplanetary dust,' submitted to *Astron. Astrophys.*
- Roettger, E.E., Feldman, P.D., A'Hearn, M.F., Festou, M.C., McFadden, L.A.M., and Gilmozzi, R., 1989, 'IUE observations of the evolution of comet Wilson (1986I): Comparison with P/Halley,' submitted to *Icarus*.
- von Roseninge, T.T., Brandt, J.C., and Farquhar, R.W., 1986, 'The International Cometary Explorer mission to comet Giacobini-Zinner,' *Science*, 232, p. 353.
- Schiffer, R., 1985, 'The effect of surface roughness on the spectral reflectance of dielectric particles. Application to the zodiacal light,' *Astron. Astrophys.* 148, p. 347.

- Simpson, J.A., Sagdeev, R.Z., Tuzzolino, A.J., Perkins, M.A., Ksanfomality, L.V., Rabinowitz, D., Lentz, G.A., Afonin, V.V., Erö, J., Keppler, E., Kosorov, J., Petrova, E., Szabó, L., and Umlauf, G., 1986, 'Dust counter and mass analyser (DUCMA) measurements of comet Halley's coma from VEGA spacecraft,' *Nature*, 321, p. 278.
- Simpson, J.A., Rabinowitz, D., Tuzzolino, A.J., Ksanfomality, L.V., and Sagdeev, R.Z., 1987, 'The dust coma of comet P/Halley: Measurements on the VEGA 1 and VEGA 2 spacecraft,' *Astron. Astrophys.*, 187, p. 742.
- Simpson, J.A., Tuzzolino, A.J., Ksanfomality, K.V., Sagdeev, R.Z., and Vaisberg, O.L., 1989, 'Confirmation of dust clusters in the coma of comet Halley,' submitted to *Adv. Space Res.*
- Tholen, D.J., Cruikshank, D.P., Hammel, H.B., Hartmann, W.K., Lark, N., and Piscitelli, J.R., 1986, 'A comparison of the continuum colours of P/Halley, other comets and asteroids,' *ESA SP-250*, Vol. III, p. 503.
- Thomas, N., and Keller, H.U., 1989, 'The colour of comet P/Halley's nucleus and dust,' *Astron. Astrophys.*, 213, p. 487.
- Vaisberg, O.L., Smirnov, V., Omelchenko, A., Gorn, L., and Iovlev, M., 1987, 'Spatial and mass distributions of low-mass dust particles ($m < 10^{-10}$ g) in comet P/Halley's coma,' *Astron. Astrophys.*, 187, p. 753.
- Veverka, J., and Noland, M., 1973, 'Asteroid reflectivities from polarisation curves: Calibration of the "slope-albedo" relationship,' *Icarus*, 19, p. 230.
- Watanabe, J., 1989, 'Rotational motion of the nucleus of comet P/Halley,' submitted to *Pub. Ast. Soc. Japan*.
- Whipple, F.L., 1958, 'The meteoric risk to space vehicles,' *Vistas in Astronautics*, Pergamon Press, p. 115.